Sweetness and light: Sugar-functionalized C^N and N^N ligands in [Ir(C^N)$_2$(N^N)]Cl complexes[†]

Cathrin D. Ertl, Fabian Brunner, Edwin C. Constable, and Catherine E. Housecroft*

Department of Chemistry, University of Basel, Spitalstrasse 51, 4056 Basel, Switzerland

E-mail: catherine.housecroft@unibas.ch

†This paper is dedicated to Rick Adams in recognition of his contributions to organometallic chemistry.
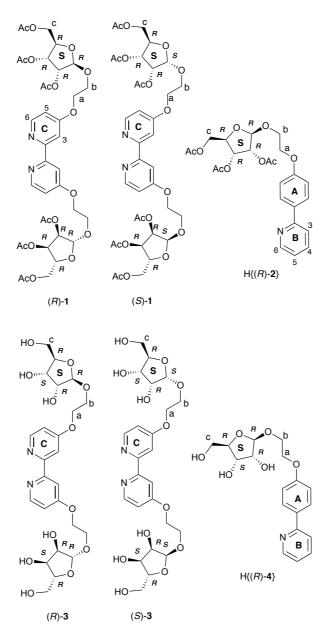
Abstract

Sugars represent a readily available entry into the chiral pool and possess a multivalent functionality allowing specific functionalzation for attachment to scaffolds possessing programmed properties. We report a series of cyclometallated iridium(III) complexes [Ir(C^N)$_2$(N^N)][PF$_6$] in which a photo- and redox-active iridium scaffold is functionalized with ribofuranose substituents. The localization of HOMO and LUMO character in different parts of the iridium core is retained in the conjugates and proof-of-concept compounds with the ribofuranose attached to the C^N and N^N ligands confirm that the photophysical and redox properties may be refined utilizing the well-established algorithms.

1. Introduction

Stereogenic ligands in metal complexes can play a number of crucial roles and one that is long investigated is in the generation of chiral reaction spaces for asymmetric catalysis [1,2,3]. Although many chiral ligands and complexes result from elegant design and synthetic strategies, the ready availability of enantiopure sugars from the chiral pool makes them attractive candidates for incorporation as stereogenic motifs. Typically, sugars contain multiple defined and enantiostable stereogenic centres together with less well defined stereochemistries at the anomeric centres. Peripheral sugar moieties as enantiopure substituents on ligands can be used for chiral induction at stereogenic metal centres in appropriate complexes [4]. Sugar functionalities are also of great interest in modifying the physicochemical properties of metal complexes, in particular the multiple hydroxy substiuents can dramatically increase the hydrophilicity of the compound, facilitating the use of such metal complexes in biological applications [5]. Finally, the introduction of biomotifs allows the use of such complexes for the delivery of unnatural functional properties to target cells or cell components using established biological molecular recognition strategies and offers new strategies for photodynamic therapies when the biomotifs are conjugated with photoactive centres. The conjugation of luminescent transition metal scaffolds with sugar domains has attracted some recent interest [6] with some focus on cyclometallated iridium(III) complexes [7,8,9,10,11] bearing . Colour tuning of $[Ir(C^\wedge N)_2(N^\wedge N)]^+$ complexes ($C^\wedge N$ = cyclometallating ligand, $N^\wedge N$ = chelating N,N'-donor) is facile and the localized nature of the highest-occupied and lowest-unoccupied molecular orbitals (HOMO and LUMO) in the ground state of the complex allows the two levels to be selectively addressed. Typically, the HOMO is localized on the $\{Ir(C^\wedge N)_2\}$ domain, whilst the LUMO is localized on the $N^\wedge N$ ligand [12]. Thus, the emission energy can be tuned by modification of the $C^\wedge N$ or the $N^\wedge N$ ligands to modify the HOMO and LUMO energy

levels respectively [12]. We have now extended our previous investigations in sugar-functionalized oligopyridine ligands [4,13,14] to include their incorporation into emissive $[Ir(C^\wedge N)_2(N^\wedge N)]^+$ complexes. We present here an investigation of the syntheses, photophysical and electrochemical properties of a series of $[Ir(C^\wedge N)_2(N^\wedge N)]Cl$ complexes incorporating the ligands shown in Scheme 1.

Scheme 1. Structures of the protected and deprotected sugar-functionalized ligands. For the ligand abbreviations, only the stereochemistry at the anomeric carbon atom is designated. Ring and atom labels for NMR spectroscopic assignments are shown.

2.   Experimental

2.1   General

All starting materials were purchased as reagent grade and used as received. For reactions performed under inert atmosphere, dry solvents were obtained from Sigma-Aldrich or Acros Organics. For all other reactions, solvents were of reagent grade or distilled. For analyses, HPLC grade solvents were used. Column chromatography was carried out with Silicycle silica gel (40–63 μm). Dowex 50WX4 was purchased from Fluka.

NMR spectra were recorded on Bruker Avance III-400 (400 MHz) and III-500 (500 MHz) spectrometers. Chemical shifts were referenced to residual solvent peaks with δ(TMS) = 0 ppm. Electrospray ionization mass spectra were measured on a Bruker esquire 3000^{plus} or a Shimadzu LCMS-2020 instrument and high resolution ESI mass spectra on a Bruker maXis 4G QTOF spectrometer. LC-ESI mass spectrometry was carried out on a combination of Shimadzu (LC) and Bruker AmaZon X instruments. Absorption spectra were obtained on an Agilent 8453 spectrophotometer and emission spectra on a Shimadzu 5301PC spectrofluorophotometer. Photoluminescence quantum yields were measured on a Hamamatsu absolute PL quantum yield spectrometer C11347 Quantaurus QY and excited-state lifetime measurements were performed on a Hamamatsu Compact Fluorescence lifetime spectrometer C11367 Quantaurus Tau.

Electrochemical measurements were carried out using a CH Instruments 900B potentiostat using propylene carbonate solutions of complexes with [^{n}Bu$_4$N][PF$_6$] (0.1 M) as supporting electrolyte and at a scan rate of 0.1 V s^{-1}. The working electrode was glassy carbon, the reference electrode was a leakless Ag^{+}/AgCl (eDAQ ET069-1) and the counter-electrode a Pt wire. Final potentials were referenced with respect to the Fc/Fc^{+} couple.

4,4'-Dihydroxy-2,2'-bipyridine [15], 2-(4-hydroxyphenyl)pyridine [16], 2-bromoethyl-2,3,5-triacetyl-β-D-ribofuranoside [4,13], (*R*)-**1** [4] and [Ir(ppy)$_2$Cl]$_2$ [17,18] were synthesized following literature procedures. 2-Bromoethyl-2,3,5-triacetyl-α-D-ribofuranoside was obtained as a side product in 9.1% yield from the synthesis of 2-bromoethyl-2,3,5-triacetyl-β-D-ribofuranoside [4,13].

*2.2   (S)-**1***

4,4'-Dihydroxy-2,2'-bipyridine (30.5 mg, 0.162 mmol, 0.54 eq.) and K$_2$CO$_3$ (127 mg, 0.919 mmol, 3.0 eq.) were suspended in dry DMF (2.5 mL) under a nitrogen atmosphere and heated to 75 °C. After 45 min, a solution of 2-bromoethyl-2,3,5-triacetyl-α-D-ribofuranoside (116 mg, 0.303 mmol, 1.0 eq.) in dry DMF (2.5 mL) and KI (50.2 mg, 0.302 mmol, 1.0 eq.) were added and heated at 75 °C overnight. The mixture was left to cool to room temperature and the solvent evaporated under reduced pressure. The residue was suspended in H$_2$O and extracted with CH$_2$Cl$_2$ (3×20 mL). The combined organic layers were dried over Na$_2$SO$_4$ and the solvent removed under reduced pressure. The crude product was purified by column chromatography (SiO$_2$, CH$_2$Cl$_2$–8% MeOH) to yield (*S*)-**1** as a colourless oil (94.6 mg, 0.119 mmol, 78.5%). ^{1}H NMR (500 MHz, CDCl$_3$) δ/ppm 8.46 (d, *J* = 5.6 Hz, 2H, H^{C6}), 7.98 (d, *J* = 2.6 Hz, 2H, H^{C3}), 6.86 (dd, *J* = 5.7, 2.6 Hz, 2H, H^{C5}), 5.37 (d, *J* = 4.5 Hz, 2H, H^{S1}), 5.17 (dd, *J* = 7.4, 4.0 Hz, 2H, H^{S3}), 4.97 (dd, *J* = 7.4, 4.5 Hz, 2H, H^{S2}), 4.39–4.28 (m, 8H, H$^{S4+a+a'+c}$), 4.21 (dd, *J* = 11.9, 4.1 Hz, 2H, H$^{c'}$), 4.10 (ddd, *J* = 11.6, 5.3, 3.7 Hz, 2H, H^{b}), 3.94 (ddd, *J* = 11.5, 6.5, 3.7 Hz, 2H, H$^{b'}$), 2.09 (s, 6H, H$^{S3-OAc/c-OAc}$), 2.08 (s, 6H, H$^{S3-OAc/c-OAc}$), 2.05 (s, 6H, H^{S2-OAc}). ^{13}C NMR (126 MHz, CDCl$_3$) δ/ppm 170.5 (2C, C$^{S3-C(O)+c-C(O)}$), 169.9 (C$^{S2-C(O)}$), 165.9 (C^{C4}), 157.8 (C^{C2}), 150.2 (C^{C6}), 111.4 (C^{C5}), 106.6 (C^{C3}), 100.8 (C^{S1}), 79.5 (C^{S4}), 70.9 (C^{S2}), 69.9 (C^{S5}), 67.1 (C^{a}), 66.5 (C^{b}), 63.5 (C^{c}), 21.0 (C$^{S3-OAc/c-OAc}$), 20.9 (C$^{S3-OAc/c-OAc}$), 20.6 (C^{S2-OAc}). LC-ESI MS *m/z* 793.3 [*M*+H]$^{+}$ (calc. 793.3).

2.3 H{(R)-2}

2-(4-Hydroxyphenyl)pyridine (67.8 mg, 0.396 mmol, 1.0 eq.) and K_2CO_3 (164 mg, 1.18 mmol, 3.0 eq.) were suspended in dry DMF (2.5 mL) under a nitrogen atmosphere and heated to 75 °C. After 45 min, a solution of 2-bromoethyl-2,3,5-triacetyl-β-D-ribofuranoside (152 mg, 0.397 mmol, 1.0 eq.) in dry DMF (2.5 mL) and KI (66.4 mg, 0.400 mmol, 1.0 eq.) were added and stirred overnight at 75 °C. The mixture was left to cool to room temperature and the solvent was evaporated under reduced pressure. The residue was suspended in H_2O (20 mL) and extracted with CH_2Cl_2 (3×20 mL). The combined organic layers were dried over Na_2SO_4 and the solvent was removed under reduced pressure. The crude product was purified by column chromatography (SiO_2, EtOAc/cyclohexane 1:1) to yield H{(R)-2} as a colourless oil (150 mg, 0.317 mmol, 80.0%). ^{1}H NMR (500 MHz, $CDCl_3$) δ/ppm 8.64 (ddd, J = 4.9, 1.9, 1.0 Hz, 1H, H^{B6}), 7.97–7.91 (m, 2H, H^{A3}), 7.71 (ddd, J = 8.1, 7.3, 1.8 Hz, 1H, H^{B4}), 7.66 (dt, J = 8.1, 1.2 Hz, 1H, H^{B3}), 7.17 (ddd, J = 7.2, 4.8, 1.3 Hz, 1H, H^{B5}), 7.02–6.97 (m, 2H, H^{A2}), 5.36 (dd, J = 6.7, 4.9 Hz, 1H, H^{S3}), 5.31 (dd, J = 4.9, 0.9 Hz, 1H, H^{S2}), 5.13 (s, 1H^{S1}), 4.39–4.30 (m, 2H, H^{S4+c}), 4.21–4.14 (m, 3H, $H^{a+a'+c'}$), 4.07 (dt, J = 11.1, 4.5 Hz, 1H, H^b), 3.85 (dt, J = 11.0, 4.8 Hz, 1H, $H^{b'}$), 2.11 (s, 3H, H^{S2-OAc}), 2.08 (s, 3H, H^{c-OAc}), 2.05 (s, 3H, H^{S3-OAc}). ^{13}C NMR (126 MHz, $CDCl_3$) δ/ppm 170.8 ($C^{c-C(O)}$), 169.80 ($C^{S3-C(O)}$), 169.75 ($C^{S2-C(O)}$), 159.6 (C^{A1}), 157.2 (C^{B1}), 149.7 (C^{B6}), 136.8 (C^{B4}), 132.5 (C^{A4}), 128.3 (C^{A3}), 121.6 (C^{B5}), 120.0 (C^{B3}), 114.9 (C^{A2}), 105.6 (C^{S1}), 78.9 (C^{S4}), 74.9 (C^{S2}), 71.7 (C^{S3}), 67.1 (C^a), 66.5 (C^b), 64.9 (C^c), 21.0 (C^{c-OAc}), 20.8 (C^{S2-OAc}), 20.7 (C^{S3-OAc}). LC-ESI MS m/z 474.2 $[M+H]^+$ (calc. 474.2).

2.4 [Ir{(R)-2}₂Cl]₂

H{(*R*)-**2**} (147 mg, 310 µmol, 1.0 eq.) was dissolved in 2-ethoxyethanol (3 mL) under nitrogen atmosphere. [Ir(cod)Cl]$_2$ (52.3 mg, 77.9 µmol, 0.25 eq.) was added and the mixture was heated at reflux overnight. A few drops of H$_2$O were added and the resulting orange precipitate was filtered off, washed with EtOH and Et$_2$O and redissolved in CH$_2$Cl$_2$. The solvent was removed under reduced pressure to yield [Ir{(*R*)-**2**}$_2$Cl]$_2$ as an orange solid which was used for subsequent transformations without further purification (70.6 mg, 30.1 µmol, 38.8%). ^{1}H NMR (400 MHz, CDCl$_3$) *δ*/ppm 9.14 (tt, *J* = 4.0, 1.1 Hz, 4H), 7.81–7.66 (m, 8H), 7.40 (d, *J* = 8.7 Hz, 4H), 6.74–6.68 (m, 4H), 6.34 (dd, *J* = 8.5, 2.5 Hz, 4H), 5.39 (t, *J* = 2.8 Hz, 4H), 5.26 (dd, *J* = 6.7, 4.9 Hz, 4H), 5.18 (ddd, *J* = 4.7, 3.3, 0.9 Hz, 4H), 4.96 (d, *J* = 1.9 Hz, 4H), 4.32–4.20 (m, 8H), 4.03 (ddd, *J* = 11.5, 5.9, 2.6 Hz, 4H), 3.81–3.71 (m, 4H), 3.66 (q, *J* = 3.7, 2.5 Hz, 8H), 3.56 (dt, *J* = 10.2, 4.9 Hz, 4H), 2.06 (s, 6H), 2.06 (s, 6H), 2.03 (s, 6H), 2.02 (s, 6H), 1.99 (s, 6H), 1.97 (s, 6H). LC-ESI-MS *m/z* 1137.3 [Ir(C^N)$_2$]$^+$ (calc. 1137.3).

2.5   General Procedure for the Synthesis of Ir(III) Complexes

Chlorido-bridged Ir(III) dimer and N^N ligand were suspended in MeOH (5 mL) and heated at reflux overnight. The suspension was left to cool to room temperature, filtered through Celite®, washed with MeOH and the filtrate was concentrated under reduced pressure. The crude product was purified by column chromatography (SiO$_2$, CH$_2$Cl$_2$– MeOH) to yield the desired product.

2.6   [Ir(ppy)$_2${(R)-1}]Cl

[Ir(ppy)$_2$Cl]$_2$ (56.0 mg, 52.2 µmol, 0.51 eq.) and (*R*)-**1** (82.0 mg, 103 µmol, 1.0 eq.). Purification by column chromatography with CH$_2$Cl$_2$–10% MeOH gave [Ir(ppy)$_2${(*R*)-**1**}]Cl as a yellow solid (122 mg, 91.8 µmol, 88.8%). ^{1}H NMR (500 MHz, CD$_3$CN) *δ*/ppm 8.30 (m, 2H, H^{C3}), 8.05 (dt, *J* = 8.2, 1.0 Hz, 2H, H^{B3}), 7.86–7.80 (m, 2H, H^{B4}),

7.78 (dd, J = 8.0, 1.3 Hz, 2H, H^{A3}), 7.70 (d, J = 6.4 Hz, 2H, H^{C6}), 7.69–7.67 (m, 2H, H^{B6}), 7.05 (ddd, J = 7.4, 5.8, 1.4 Hz, 2H, H^{B5}), 7.02–6.99 (m, 4H, H^{A4+C5}), 6.88 (td, J = 7.4, 1.3 Hz, 2H, H^{A5}), 6.27 (dd, J = 7.6, 1.2 Hz, 2H, H^{A6}), 5.17 (dd, J = 6.5, 4.7 Hz, 2H, H^{S3}), 5.14–5.09 (m, 4H, H^{S1+S2}), 4.50–4.40 (m, 4H, $H^{a+a'}$), 4.31–4.25 (m, 4H, H^{S4+c}), 4.12–4.07 (m, 2H, $H^{c'}$), 4.07–4.00 (m, 2H, H^{b}), 3.87–3.80 (m, 2H, $H^{b'}$), 2.05 (s, 3H, H^{c-OAc}), 2.04 (s, 3H, H^{c-OAc*}), 2.00 (s, 6H, H^{S3-OAc}), 1.98 (s, 3H, H^{S2-OAc}), 1.97 (s, 3H, $H^{S2-OAc*}$). ^{13}C NMR (126 MHz, CD$_3$CN) δ/ppm 171.50 ($C^{c-C(O)}$), 171.49 ($C^{c-C(O)*}$), 170.8 ($C^{S3-C(O)}$), 170.64 ($C^{S2-C(O)}$), 170.63 ($C^{S2-C(O)*}$), 168.4 (C^{B2}), 168.0 (C^{C4}), 158.4 (C^{C2}), 152.2 (C^{C6}), 151.8 (C^{A1}), 150.0 (C^{B6}), 145.1 (C^{A2}), 139.2 (C^{B4}), 132.5 (C^{A6}), 131.2 (C^{A5}), 125.7 (C^{A3}), 124.3 (C^{B5}), 123.2 (C^{A4}), 120.6 (C^{B3}), 115.4 (C^{C5}), 112.81 (C^{C3}), 112.79 (C^{C3*}), 106.01 (C^{S1}), 105.97 (C^{S1*}), 79.4 (C^{S4}), 75.1 (C^{S2}), 72.6 (C^{S3}), 69.8 (C^{a}), 66.5 (C^{b}), 66.4 (C^{b*}), 65.60 (C^{c}), 65.57 (C^{c*}), 21.0 (C^{S2-OAc}), 20.73 (C^{c-OAc}), 20.66 (C^{S3-OAc}). ESI MS m/z 1293.8 [M–Cl]$^+$ (calc. 1293.4). HR ESI-MS m/z 1293.3537 [M–Cl]+ (calc. 1293.3531). UV-Vis (MeOH, 1.0×10^{-5} M) λ/nm (ε/dm^3 mol^{-1} cm^{-1}) 223 (50 500), 255 (57 700), 300 sh (21 400), 342 sh (9600), 412 sh (3700). Emission (MeOH, 1.0×10^{-5} M, λ_{exc} = 380 nm) λ_{em}^{max} = 571 nm.

2.7 [Ir(ppy)$_2${(S)-**1**}]Cl

[Ir(ppy)$_2$Cl]$_2$ (64.0 mg, 59.7 μmol, 0.51 eq.) and (S)-**1** (93.3 mg, 118 μmol, 1.0 eq.). Purification by column chromatography with CH$_2$Cl$_2$–10% MeOH gave [Ir(ppy)$_2${(S)-**1**}]Cl as a yellow solid (123 mg, 92.6 μmol, 78.2%). ^{1}H NMR (500 MHz, CD$_3$CN) δ/ppm 8.11 (dd, J = 2.5, 1.7 Hz, 2H, H^{C3}), 8.05 (dt, J = 8.2, 1.2 Hz, 2H, H^{B3}), 7.84 (ddd, J = 8.3, 7.5, 1.5 Hz, 2H, H^{B4}), 7.78 (dd, J = 7.9, 1.2 Hz, 2H, H^{A3}), 7.73 (dd, J = 6.4, 2.4 Hz, 2H, H^{C6}), 7.65 (dddd, J = 7.3, 5.9, 1.6, 0.7 Hz, 2H, H^{B6}), 7.09–7.00 (m, 6H, $H^{A4+B5+C5}$), 6.89 (td, J = 7.4, 1.3 Hz, 2H, H^{A5}), 6.27 (ddd, J = 7.7, 2.4, 1.2 Hz, 2H, H^{A6}), 5.29 (t, J = 4.5 Hz, 2H, H^{S1}), 5.09 (dd, J = 7.4, 4.2 Hz, 2H, H^{S3}), 4.96 (ddd, J = 9.8, 7.4,

4.5 Hz, 2H, H^{S2}), 4.40 (dt, J = 7.1, 3.8 Hz, 4H, $H^{a+a'}$), 4.26 (dd, J = 11.9, 3.2 Hz, 2H, H^c), 4.21 (dtd, J = 7.7, 4.4, 3.2 Hz, 2H, H^{S4}), 4.12 (dt, J = 11.8, 4.3 Hz, 2H, $H^{c'}$), 4.07–4.00 (m, 2H, H^b), 3.93–3.85 (m, 2H, $H^{b'}$), 1.99 (s, 3H, $H^{c\text{-}OAc}$), 1.98 (s, 3H, $H^{c\text{-}OAc*}$), 1.92 (s, 3H, $H^{S3\text{-}OAc}$), 1.91 (s, 3H, $H^{S3\text{-}OAc*}$), 1.90 (s, 3H, $H^{S2\text{-}OAc}$), 1.80 (s, 3H, $H^{S2\text{-}OAc*}$). ^{13}C NMR (126 MHz, CD$_3$CN) δ/ppm 171.3 ($C^{c\text{-}C(O)}$), 171.0 ($C^{S3\text{-}C(O)}$), 170.51 ($C^{S2\text{-}C(O)}$), 170.45 ($C^{S2\text{-}C(O)*}$), 168.55 (C^{B2}), 168.53 (C^{B2*}), 168.14 (C^{C4}), 168.10 (C^{C4*}), 158.3 (C^{C2}), 152.4 (C^{C6}), 151.7 (C^{A1}), 149.9 (C^{B6}), 145.1 (C^{A2}), 139.3 (C^{B4}), 132.53 (C^{A6}), 132.50 (C^{A6*}), 131.2 (C^{A5}), 125.8 (C^{A3}), 124.3 (C^{B5}), 123.3 (C^{A4}), 120.7 (C^{B3}), 115.43 (C^{C5}), 115.40 (C^{C5*}), 112.8 (C^{C3}), 101.7 (C^{S1}), 101.6 (C^{S1*}), 80.3 (C^{S4}), 71.5 (C^{S2}), 70.4 (C^{S3}), 70.14 (C^a), 70.10 (C^{a*}), 66.9 (C^b), 64.1 (C^c), 20.90 ($C^{c\text{-}OAc}$), 20.89 ($C^{c\text{-}OAc*}$), 20.85 ($C^{S3\text{-}OAc}$), 20.8 ($C^{S3\text{-}OAc*}$), 20.6 ($C^{S2\text{-}OAc}$), 20.5 ($C^{S2\text{-}OAc*}$). ESI MS m/z 1293.7 $[M–Cl]^+$ (calc. 1293.4). HR ESI MS m/z 1293.3541 $[M–Cl]^+$ (calc. 1293.3531). UV-Vis (MeOH, 1.0 × 10^{-5} M) λ/nm (ε/dm^3 mol^{-1} cm^{-1}) 223 (48 700), 255 (55 100), 300 sh (21 000), 342 sh (9400), 412 sh (3300). Emission (MeOH, 1.0 × 10^{-5} M, λ_{exc} = 380 nm) λ_{em}^{max} = 576 nm.

2.8 *[Ir{(R)-**2**}₂(bpy)]Cl*

[Ir{(R)-**2**}$_2$Cl]$_2$ (70.6 mg, 30.1 µmol, 1.0 eq.) and bpy (10.2 mg, 65.3 µmol, 2.2 eq.). Purification by column chromatography with CH$_2$Cl$_2$–10% MeOH changing to CH$_2$Cl$_2$–20% MeOH gave [Ir{(R)-**2**}$_2$(bpy)]Cl as a yellow solid (36.7 mg, 27.6 µmol, 45.9%). ^{1}H NMR (500 MHz, CD$_3$CN) δ/ppm 8.59 (d, J = 8.0 Hz, 2H, H^{C3}), 8.13 (td, J = 7.9, 1.7 Hz, 2H, H^{C4}), 8.04 (dt, J = 5.3, 1.8 Hz, 2H, H^{C6}), 7.93 (dt, J = 8.3, 1.1 Hz, 2H, H^{B3}), 7.81–7.71 (m, 4H, H^{A3+B4}), 7.56–7.48 (m, 4H, H^{B6+C5}), 6.93 (dddd, J = 7.3, 5.8, 2.7, 1.4 Hz, 2H, H^{B5}), 6.63 (ddd, J = 8.7, 2.6, 0.9 Hz, 2H, H^{A4}), 5.72 (dd, J = 2.6, 1.4 Hz, 2H, H^{A6}), 5.15 (ddd, J = 6.7, 4.9, 2.8 Hz, 2H, H^{S3}), 5.09 (dd, J = 4.9, 1.0 Hz, 2H, H^{S2}), 5.01 (t, J = 1.0 Hz, 2H, H^{S1}), 4.30–4.20 (m, 4H, H^{S4+c}), 4.01 (dt, J = 11.5, 5.5 Hz, 2H, $H^{c'}$), 3.90 (ddd, J = 7.6, 5.8, 3.6 Hz, 4H, $H^{a+a'}$), 3.87–3.81 (m, 2H, H^b), 3.63 (dtd, J = 11.5, 6.0, 3.2

Hz, 2H, $H^{b'}$), 2.05 (s, 3H, H^{S2-OAc}), 2.04 (s, 3H, $H^{S2-OAc*}$), 2.00 (s, 3H, H^{S3-OAc}), 2.00 (s, 3H, $H^{S3-OAc*}$), 1.96 (s, 3H, H^{c-OAc}), 1.94 (s, 3H, H^{c-OAc*}). ^{13}C NMR (126 MHz, CD$_3$CN) δ/ppm 171.27 ($C^{c-C(O)}$), 171.25 ($C^{c-C(O)*}$), 170.9 ($C^{S3-C(O)}$), 170.6 ($C^{S2-C(O)}$), 168.07 (C^{B2}), 168.05 (C^{B2*}), 161.16 (C^{A5}), 161.15 (C^{A5*}), 156.7 (C^{C2}), 153.7 (C^{A1}), 153.6 (C^{A1*}), 151.7 (C^{C6}), 149.9 (C^{B6}), 140.3 (C^{C4}), 139.3 (C^{B4}), 138.00 (C^{A2}), 137.98 (C^{A2*}), 129.3 (C^{C5}), 127.6 (C^{A3}), 125.7 (C^{C3}), 123.20 (C^{B5}), 123.18 (C^{B5*}), 120.1 (C^{B3}), 118.0 (C^{A6}), 117.9 (C^{A6*}), 109.2 (C^{A4}), 109.0 (C^{A4*}), 106.0 (C^{S1}), 105.9 (C^{S1*}), 79.4 (C^{S4}), 79.3 (C^{S4*}), 75.19 (C^{S2}), 75.18 (C^{S2*}), 72.3 (C^{S3}), 72.2 (C^{S3*}), 67.39 (C^a), 67.37 (C^{a*}), 66.94 (C^b), 66.85 (C^{b*}), 65.0 (C^c), 64.8 (C^{c*}), 21.00 (C^{c-OAc}), 20.98 (C^{c-OAc*}), 20.75 (C^{S2-OAc}), 20.74 ($C^{S2-OAc*}$), 20.69 (C^{S3-OAc}). ESI MS m/z 1293.2 [M–Cl]$^+$ (calc. 1293.4). HR ESI-MS m/z 1293.3535 (calc. 1293.3526). UV-Vis (MeOH, 1.0×10^{-5} M) λ/nm (ε/dm^3 mol^{-1} cm^{-1}) 253 (47 300), 276 (55 500), 310 sh (36 300), 370 sh (10 700). Emission (MeOH, 1.0×10^{-5} M, $\lambda_{\text{exc}} = 380$ nm) $\lambda_{em}^{max} = 588$ nm.

2.9   General procedure for deprotection of acetyl-protected Ir(III) complexes

NaOMe was added to a solution of acetyl-protected Ir(III) complex in MeOH (2–10 mL) and stirred at room temperature for 4–8 h. Acidic DOWEX 50WX4 (pre-washed with H$_2$O, 1 M HCl, H$_2$O, MeOH) was added and the mixture was stirred at room temperature for 30 min. The mixture was filtered through Celite® and the filtrate was concentrated under reduced pressure. The residue was washed with acetone and dried under vacuum to yield the desired product.

2.10   [Ir(ppy)$_2${(R)-3}]Cl

[Ir(ppy)$_2${(R)-**1**}]Cl (122 mg, 91.8 μmol, 1.0 eq.) and NaOMe (5.30 mg, 96.1 μmol, 1.1 eq.) in MeOH (10 mL), stirring for 4 h. [Ir(ppy)$_2${(R)-**3**}]Cl was obtained as a yellow solid (97.4 mg, 90.5 μmol, 98.6%). ^{1}H NMR (500 MHz, DMSO-d$_6$) δ/ppm 8.49 (t, $J =$

2.9 Hz, 2H, H^{C3}), 8.24 (dt, J = 8.3, 1.0 Hz, 2H, H^{B3}), 7.95–7.91 (m, 2H, H^{B4}), 7.89 (dd, J = 7.8, 1.3 Hz, 2H, H^{A3}), 7.71–7.64 (m, 2H, H^{B6}), 7.59 (d, J = 6.4 Hz, 2H, H^{C6}), 7.28 (dd, J = 6.5, 2.6 Hz, 2H, H^{C5}), 7.18 (ddd, J = 7.3, 5.7, 1.4 Hz, 2H, H^{B5}), 6.99 (td, J = 7.5, 1.2 Hz, 2H, H^{A4}), 6.87 (td, J = 7.4, 1.3 Hz, 2H, H^{A5}), 6.19 (dd, J = 7.6, 1.2 Hz, 2H, H^{A6}), 4.83 (s, 2H, H^{S1}), 4.43–4.31 (m, 4H, $H^{a+a'}$), 3.96 (ddd, J = 11.9, 5.1, 3.1 Hz, 2H, H^{b}), 3.86–3.80 (m, 2H, H^{S3}), 3.80–3.72 (m, 4H, $H^{S4+b'}$), 3.71 (dt, J = 4.7, 1.2 Hz, 2H, H^{S2}), 3.51 (dt, J = 11.6, 3.9 Hz, 2H, H^{c}), 3.33 (dt, J = 11.6, 5.9 Hz, 8H, $H^{c'+S2-OH+S3-OH+c-OH}$).
^{13}C NMR (126 MHz, DMSO-d6) δ/ppm 166.9 (C^{B2}), 166.2 (C^{C4}), 156.9 (C^{C2}), 151.1 (C^{A1}), 150.5 (C^{C6}), 148.8 (C^{B6}), 143.9 (C^{A2}), 138.5 (C^{B4}), 131.2 (C^{A6}), 130.1 (C^{A5}), 125.0 (C^{A3}), 123.8 (C^{B5}), 122.0 (C^{A4}), 119.9 (C^{B3}), 114.9 (C^{C5}), 111.9 (C^{C3}), 106.89 (C^{S1}), 106.87 (C^{S1*}), 83.8 (C^{S4}), 74.3 (C^{S2}), 70.9 (C^{S3}), 68.7 (C^{a}), 64.5 (C^{b}), 63.0 (C^{c}). ESI MS m/z 1041.2 [M–Cl]$^{+}$ (calc. 1041.3). HR ESI-MS m/z 1041.2887 [M–Cl]+ (calc. 1041.2896). UV-Vis (MeOH, 1.0×10^{-5} M) λ/nm (ε/dm^3 mol^{-1} cm^{-1}) 223 (48 300), 255 (55 800), 300 sh (21 100), 342 sh (9600), 412 sh (3500). Emission (MeOH, 1.0×10^{-5} M, λ_{exc} = 380 nm) λ_{em}^{max} = 572 nm.

2.11   *[Ir(ppy)₂{(S)-3}]Cl*

[Ir(ppy)$_2${(S)-**1**}]Cl (70.0 mg, 52.7 µmol, 1.0 eq.) and NaOMe (2.90 mg, 52.7 µmol, 1.0 eq.) in MeOH (6 mL), stirring for 5 h. [Ir(ppy)$_2${(S)-**3**}]Cl was obtained as a yellow solid (54.9 mg, 51.0 µmol, 96.8%). ^{1}H NMR (500 MHz, DMSO-d6) δ/ppm 8.50 (s, 2H, H^{C3}), 8.24 (dt, J = 8.3, 0.9 Hz, 2H, H^{B3}), 7.94–7.90 (m, 2H, H^{B4}), 7.89 (dd, J = 8.0, 1.3 Hz, 2H, H^{A3}), 7.70–7.65 (m, 2H, H^{B6}), 7.59 (d, J = 6.4 Hz, 2H, H^{C6}), 7.29 (dd, J = 6.5, 2.6 Hz, 2H, H^{C5}), 7.18 (ddd, J = 7.3, 5.8, 1.4 Hz, 2H, H^{B5}), 6.99 (td, J = 7.5, 1.2 Hz, 2H, H^{A4}), 6.87 (td, J = 7.5, 1.3 Hz, 2H, H^{A5}), 6.19 (dd, J = 7.6, 1.2 Hz, 2H, H^{A6}), 4.95 (dd, J = 4.4, 1.1 Hz, 2H, H^{S1}), 4.72 (br, 2H, H^{c-OH}), 4.57 (br, 2H, H^{S3-OH}), 4.48–4.36 (m, 4H, $H^{a+a'}$), 4.17 (br, 2H, H^{S2-OH}), 4.02–3.93 (m, 2H, H^{b}), 3.89–3.78 (m, 6H, $H^{S2+S4+b'}$), 3.78–

3.72 (br, 2H, H^{S3}), 3.45–3.36 (br, 4H, $H^{c+c'}$). ^{13}C NMR (126 MHz, DMSO-d6) δ/ppm 166.9 (C^{B2}), 166.7 (C^{C4}), 156.9 (C^{C2}), 151.0 (C^{A1}), 150.3 (C^{C6}), 148.6 (C^{B6}), 143.8 (C^{A2}), 138.4 (C^{B4}), 131.0 (C^{A6}), 129.9 (C^{A5}), 124.9 (C^{A3}), 123.7 (C^{B5}), 121.8 (C^{A4}), 119.7 (C^{B3}), 114.7 (C^{C5}), 111.7 (C^{C3}), 101.7 (C^{S1}), 84.9 (C^{S4}), 70.9 (C^{S2}), 69.0 (C^{S3}), 68.7 (C^{a}), 65.1 (C^{b}), 61.4 (C^{c}). ESI MS m/z 1041.1 $[M\text{–}Cl]^+$ (calc. 1041.3). HR ESI-MS m/z 1041.2897 (calc. 1041.2896). UV-Vis (MeOH, 1.0×10^{-5} M) λ/nm (ε/dm^3 mol^{-1} cm^{-1}) 223 (48 200), 255 (55 600), 300 sh (21 200), 342 sh (9700), 412 sh (3600). Emission (MeOH, 1.0×10^{-5} M, λ_{exc} = 380 nm) λ_{em}^{max} = 572 nm.
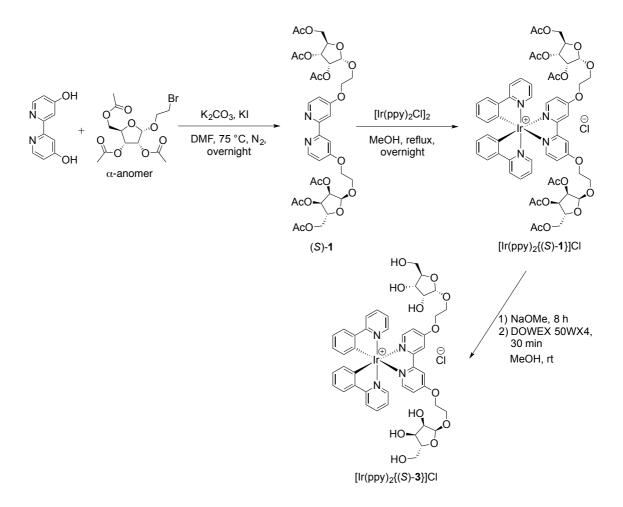
2.12 [Ir{(R)-4}₂(bpy)]Cl

[Ir{(R)-**2**}$_2$(bpy)]Cl (18.4 mg, 13.8 μmol, 1.0 eq.) and NaOMe (0.84 mg, 15.2 μmol, 1.1 eq.) in MeOH (2 mL), stirring for 8 h. [Ir{(R)-**4**}$_2$(bpy)]Cl was obtained as a yellow solid (12.4 mg, 11.5 μmol, 83.5%). ^{1}H NMR (500 MHz, DMSO-d6) δ/ppm 8.88 (d, J = 8.2 Hz, 2H, H^{C3}), 8.27 (td, J = 7.9, 1.6 Hz, 2H, H^{C4}), 8.13 (d, J = 8.3 Hz, 2H, H^{B3}), 7.93 (ddd, J = 5.3, 3.5, 1.5 Hz, 2H, H^{C6}), 7.90–7.83 (m, 4H, H^{A3+B4}), 7.71 (ddd, J = 7.9, 5.5, 1.3 Hz, 2H, H^{C5}), 7.51 (dd, J = 5.8, 1.6 Hz, 2H, H^{B6}), 7.06 (ddd, J = 7.3, 5.7, 1.4 Hz, 2H, H^{B5}), 6.65 (ddd, J = 8.6, 2.7, 1.1 Hz, 2H, H^{A4}), 5.63 (d, J = 2.4 Hz, 2H, H^{A6}), 5.03 (br, 2H, $H^{S2\text{-}OH}$), 4.85 (br, 2H, $H^{S3\text{-}OH}$), 4.74 (s, 2H, H^{S1}), 4.52 (br, 2H, $H^{c\text{-}OH}$), 3.94–3.71 (m, 10H, $H^{S3+S4+a+a'+b}$), 3.68 (d, J = 4.0 Hz, 2H, H^{S2}), 3.60–3.52 (m, 2H, $H^{b'}$), 3.50–3.44 (m, 2H, H^{c}), 3.31–3.28 (br, 2H, $H^{c'}$). ^{13}C NMR (126 MHz, DMSO-d6) δ/ppm 166.6 (C^{B2}), 159.7 (C^{A5}), 155.4 (C^{C2}), 152.6 (C^{A1}), 149.9 (C^{C6}), 148.4 (C^{B6}), 139.6 (C^{C4}), 138.5 (C^{B4}), 136.7 (C^{A2}), 128.6 (C^{C5}), 126.7 (C^{A3}), 124.9 (C^{C3}), 122.4 (C^{B5}), 119.2 (C^{B3}), 117.0 (C^{A6}), 107.4 (C^{A4}), 106.8 (C^{S1}), 83.6 (C^{S4}), 74.2 (C^{S2}), 70.7 (C^{S3}), 66.1 (C^{a}), 64.8 (C^{b}), 62.9 (C^{c}). ESI MS m/z 1041.2 $[M\text{–}Cl]^+$ (calc. 1041.3). HR ESI-MS m/z 1041.2889 [M-Cl]+ (calc. 1041.2896). UV-Vis (MeOH, 1.0×10^{-5} M) λ/nm (ε/dm^3 mol^{-1} cm^{-1}) 254

(44100), 276 (52 000), 310 sh (33 300), 370 sh (9700). Emission (MeOH, 1.0×10^{-5} M, $\lambda_{\text{exc}} = 380$ nm) $\lambda_{em}^{max} = 589$ nm.

3   *Results and discussion*

3.1   *Ligand synthesis*

For these proof of concept studies, we selected protected and deprotected sugars in the pentose series as these are both readily accessible and robust. We have previously described the synthesis of the acetyl-protected ribofuranose-functionalized bpy ligand (*R*)-**1** (Scheme 1) [4], and the anomeric ligand (*S*)-**1** was prepared by an analogous route as shown in the first step in Scheme 2 (we use an abbreviated stereochemical nomenclature to indicate the stereochemistry at the anomeric centre). A parent peak at *m/z* 793.3 in the LC-ESI mass spectrum of (*S*)-**1** was assigned to the [M+H]$^+$ ion. The solution ^{1}H and ^{13}C NMR spectra of (*S*)-**1** were consistent with a symmetrical substitution pattern of the bpy metal-binding domain, and were fully assigned using COSY, HMQC and HMBC methods; ring and atom labelling is shown in Scheme 1. The signal for proton H^{S1} at the anomeric centre appears as a singlet in (*R*)-**1** (β-configuration) [4] and as a doublet (*J* = 4.5 Hz) in (*S*)-**1** (α-configuration) with the difference in the ^3J coupling constant following the expected trend from the Karplus equation [19]. The 2-phenylpyridine derivative H{(*R*)-**2**} was prepared as shown in Scheme 3, following a similar approach to that used for (*R*)-**1**. In the LC-ESI mass spectrum, a peak at *m/z* = 474.2 was assigned to the [M+H]$^+$ ion. The solution ^{1}H and ^{13}C NMR spectra were fully assigned by 2D methods, and retention of stereochemistry at the anomeric position (β-configuration) was confirmed by the observation of a singlet for proton H^{S1}.
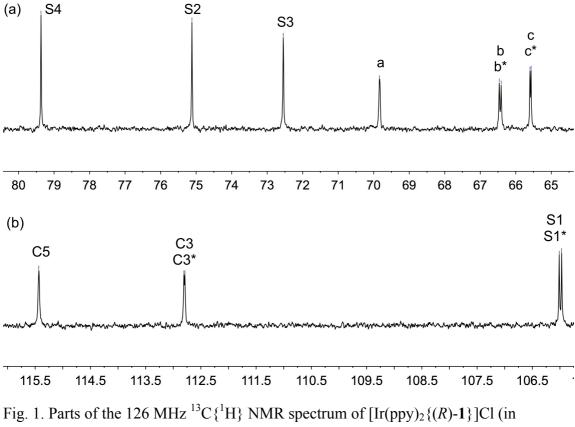
Scheme 2. Synthetic route adopted for the ribofuranose-functionalized complexes [Ir(ppy)$_2${(S)-**1**}]Cl and [Ir(ppy)$_2${(S)-**3**}]Cl.

3.2   Synthesis of [Ir(ppy)$_2${(S)-**1**}]Cl, [Ir(ppy)$_2${(R)-**1**}]Cl, [Ir(ppy)$_2${(S)-**3**}]Cl and [Ir(ppy)$_2${(R)-**3**}]Cl
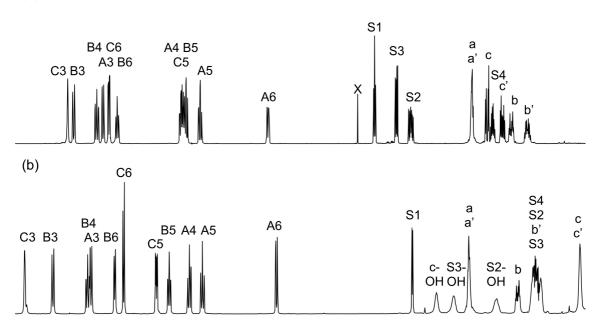
The standard methodology for the preparation of cyclometallated [Ir(C^N)$_2$(N^N)]$^+$ complexes is the treatment of a dichlorido-bridged dimer [Ir(C^N)$_2$Cl]$_2$ with an appropriate N^N ligand [17,18]. In this work, two types of [Ir(C^N)$_2$(N^N)]$^+$ complexes have been prepared, the first with the ribofuranose-functionality on the N^N bpy ligand and the second with the sugar attached to the C^N cyclometallating ligand. For the synthesis of the first series of compounds, the enantiomerically pure ligands (S)-**1** and (R)-**1** were reacted with [Ir(ppy)$_2$Cl]$_2$ (Scheme 2) and the products [Ir(ppy)$_2${(S)-**1**}]Cl and [Ir(ppy)$_2${(R)-**1**}]Cl were obtained in 78.2 and 88.8% yields, respectively. The high-

resolution electrospray mass spectra of [Ir(ppy)$_2${(S)-**1**}]Cl and [Ir(ppy)$_2${(R)-**1**}]Cl showed, respectively, peak envelopes at *m/z* 1293.3541 and 1293.3537, arising from the [M–Cl]$^+$ ion.

COSY, HMQC and HMBC techniques were used to assign the ^{1}H and ^{13}C NMR spectra of [Ir(ppy)$_2${(S)-**1**}]Cl and [Ir(ppy)$_2${(R)-**1**}]Cl. The ^{1}H and ^{13}C NMR spectra are given in Figs. S1–S4. The presence of the stereogenic {Ir(trischelate)} centre leads to each of [Ir(ppy)$_2${(S)-**1**}]$^+$ and [Ir(ppy)$_2${(R)-**1**}]$^+$ existing as a mixture of Δ and Λ diastereoisomers [20]. Typically, two signals were observed in the ^{13}C NMR spectra for nuclei close to the anomeric centre of the acetyl-protected ribofuranose functionality (Fig. 1). In the experimental section and in Fig. 1, these are distinguished by use of an asterisk, although we note that the set of signals marked with asterisks do not necessarily belong to the diastereoisomers with the same absolute Δ or Λ configurations. The relative intensities of the signals for the pairs $C^{b/b*}$, $C^{c/c*}$, $C^{S1/S1*}$ and $C^{C3/C3*}$ confirm a statistical 1:1 mixture of Δ or Λ diastereoisomers. The acetyl protecting groups are characterized by six singlets in [Ir(ppy)$_2${(S)-**1**}]Cl arising from the two diastereoisomers. In the ^{13}C NMR spectrum of [Ir(ppy)$_2${(R)-**1**}]Cl, the acetyl groups give rise only to five signal, since there is no separation of the signals arising from the acetyl groups attached to C^{S3} and C^{S3*}.

Fig. 1. Parts of the 126 MHz ^{13}C{^{1}H} NMR spectrum of [Ir(ppy)$_2${(R)-**1**}]Cl (in CD$_3$CN) showing distinction between Δ or Λ diastereoisomers for ^{13}C nuclei b, c, S1 and C3 (see Scheme 1 for numbering).

Deprotection of [Ir(ppy)$_2${(R)-**1**}]Cl and [Ir(ppy)$_2${(S)-**1**}]Cl was carried out using NaOMe [13] followed by treatment with acidic Dowex ion exchange resin to give [Ir(ppy)$_2${(R)-**3**}]Cl and [Ir(ppy)$_2${(S)-**3**}]Cl. NMR spectra of the products are given in Figs. S5–S8. Complete loss of the acetyl groups was confirmed by the disappearance of all the signals in the range δ 1.97–2.05 ppm. Figure 2 compares the solution ^{1}H NMR spectra of [Ir(ppy)$_2${(S)-**1**}]Cl and [Ir(ppy)$_2${(S)-**3**}]Cl; for reasons of solubility, a common solvent could not be used. As expected, resonances in the aliphatic region are the most affected. The ^{13}C NMR spectra of DMSO-d$_6$ solutions of the compounds were not as well resolved as those of the acetyl-protected analogs, and the only signal that showed a distinction between the Δ or Λ diastereoisomers was that for C^{S1} in [Ir(ppy)$_2${(R)-**3**}]Cl (signals at δ 106.89 and 106.87 ppm). The ESI mass spectra of

[Ir(ppy)$_2${(R)-3}]Cl and [Ir(ppy)$_2${(S)-3}]Cl exhibited peak envelopes centred at *m/z* 1041.2 and 1041.1, respectively. The isotope patterns matched those simulated for the [Ir(ppy)$_2${(R)-3}]$^+$ or [Ir(ppy)$_2${(S)-3}]$^+$ ions.
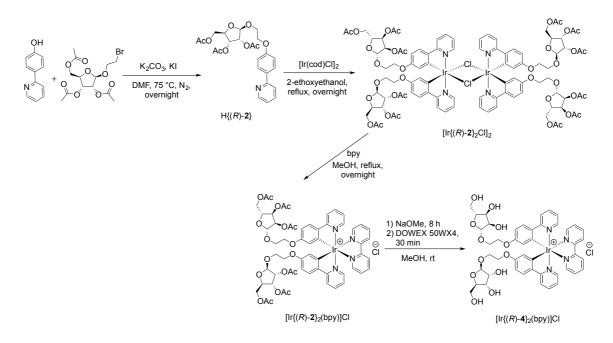
(a)

(b)

Fig. 2. Comparison of the parts of the 500 MHz ^{1}H NMR spectra of (a) [Ir(ppy)$_2${(S)-1}]Cl in CD$_3$CN, and (b) [Ir(ppy)$_2${(S)-3}]Cl in DMSO-d$_6$. × = residual CH$_2$Cl$_2$.

3.2   Synthesis of [Ir{(R)-2}$_2$(bpy)]Cl and [Ir{(R)-4}$_2$(bpy)]Cl

For the synthesis of complexes with the ribofuranose-functionality appended to the cyclometallating ligand, it was first necessary to prepare the dinuclear complex [Ir{(R)-2}$_2$Cl]$_2$. Most often, [Ir(C^N)$_2$Cl]$_2$ dimers are synthesized by treating IrCl$_3$·xH$_2$O with the appropriate H(C^N) ligand under reflux conditions [18]. However, an alternative approach starting from [Ir(cod)Cl]$_2$ [21, 22] (cod = cycloocta-1,5-diene) is sometimes more convenient and this proved to be the case for [Ir{(R)-2}$_2$Cl]$_2$ which was prepared in a one-pot quadruple cyclometallation reaction of [Ir(cod)Cl]$_2$ with H{(R)-2} (Scheme

3). In the LC-ESI mass spectrum of $[Ir\{(R)\text{-}2\}_2Cl]_2$, a peak envelope at m/z 1137.3 was observed corresponding to the $[Ir\{(R)\text{-}2\}_2]^+$ ion. ^{1}H NMR spectroscopic data were consistent with the structure shown in Scheme 3.

Scheme 3. Synthetic route to $[Ir\{(R)\text{-}2\}_2Cl]_2$, $[Ir\{(R)\text{-}2\}_2(bpy)]Cl$ and $[Ir\{(R)\text{-}4\}_2(bpy)]Cl$.

The reaction of $[Ir\{(R)\text{-}2\}_2Cl]_2$ with two equivalents of bpy yielded, after workup, yellow $[Ir\{(R)\text{-}2\}_2(bpy)]Cl$ in 45.9% yield. The high-resolution ESI-MS exhibited a peak envelope at m/z 1293.3535 arising from the $[M–Cl]^+$ ion. The solution ^{1}H and ^{13}C NMR spectra (see Figs. S9 and S10) were assigned using 2D methods, and the presence of the two diastereoisomers of the $[Ir\{(R)\text{-}2\}_2(bpy)]^+$ cation resulted in the appearance of 1:1 pairs of signals in the ^{13}C NMR spectrum for $C^{c\text{-}CO}$, C^{B2}, C^{B5}, C^{A1}, C^{A2}, C^{A4}, C^{A5}, C^{A6}, C^{S1}, C^{S2}, C^{S3}, C^{S4}, C^a, C^b, C^c, $C^{c\text{-}OAc}$ and $C^{S2\text{-}OAc}$ (see experimental section). The conversion of $[Ir\{(R)\text{-}2\}_2(bpy)]Cl$ to $[Ir\{(R)\text{-}4\}_2(bpy)]Cl$ was carried out using NaOMe as described above, and this step yielded $[Ir\{(R)\text{-}4\}_2(bpy)]Cl$ in 83.5% yield. NMR spectra of $[Ir\{(R)\text{-}4\}_2(bpy)]Cl$ are shown in Figs. S11 and S12. Loss of the acetyl resonances in the ^{1}H and ^{13}C NMR spectra confirmed complete deprotection had occurred; the OH groups in $[Ir\{(R)\text{-}4\}_2(bpy)]Cl$ gave rise to broad signals at δ 5.03, 4.85

and 4.52 ppm. Just as was observed on going from [Ir(ppy)$_2${(S)-**1**}]Cl to [Ir(ppy)$_2${(S)-**3**}]Cl in Fig. 2, the ^{1}H NMR resonances for H^{S1}, H^{S2}, H^{S3}, H^{S4} and H$^{c/c'}$ shifted to lower frequency upon deprotection, albeit with the change in solvent necessitated by the different solubility characteristics.

3.3   Electrochemical properties

The iridium(III) compounds are redox active and their electrochemical behaviour was studied by cyclic voltammetry; propylene carbonate was chosen as solvent to permit use of a common solvent for all compounds. The electrochemical data are summarized in Table 1, and a representative cyclic voltammogram is shown in Fig. 3. Each complex undergoes an oxidative process at a potential in the range +0.79 to +0.84 V with respect to the Fc/Fc$^+$ couple. These values are similar to the potential (+0.84 V) at which the parent complex [Ir(ppy)$_2$(bpy)]$^+$ undergoes a reversible oxidation (in DMF solution) [23]. Each complex undergoes a reversible, ligand-centred reduction process within the solvent window. As expected, the first reduction is at lower potential when the ribofuranose-functionality is attached to the bpy rather than the cyclometallating ligand, consistent with the substituent influencing the LUMO of the complex, which is the electrochemically addressed energy level.

Table 1. Cyclic voltammetric data referenced to Fc/Fc$^+$; propylene carbonate solutions with [^{n}Bu$_4$N][PF$_6$] supporting electrolyte, and a scan rate of 0.1 V s^{-1} (ir = irreversible).

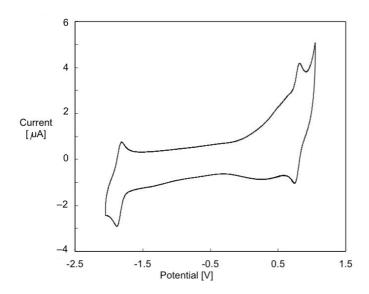| Compound	$E^{ox}_{1/2}$/V ($E_{pc} - E_{pa}$/mV)	$E^{red}_{1/2}$/V ($E_{pc} - E_{pa}$/mV)	ΔE ($E^{ox}_{1/2} - E^{red}_{1/2}$) / V
[Ir(ppy)$_2${(R)-**1**}]Cl	+0.80 (70)	−1.84 (75)	2.64
[Ir(ppy)$_2${(S)-**1**}]Cl	+0.82 (48)	−1.83 (57)	2.65
[Ir{(R)-**2**}$_2$(bpy)]Cl	+0.84 (ir)	−1.75 (74)	2.59
[Ir(ppy)$_2${(R)-**3**}]Cl	+0.80 (65)	−1.84 (86)	2.64
[Ir(ppy)$_2${(S)-**3**}]Cl	+0.79 (66)	−1.85 (86)	2.64
[Ir{(R)-**4**}$_2$(bpy)]Cl	+0.83 (ir)	−1.74 (55)	2.57

Fig. 3. Cyclic voltammogram of $[Ir(ppy)_2\{(S)$-**3**$\}]Cl$ in propylene carbonate with $[^nBu_4N][PF_6]$ supporting electrolyte, and scan rate of 0.1 V s^{-1}. Referenced with respect to Fc/Fc$^+$.

3.4 Absorption and emission spectroscopic properties

The solution absorption spectra of the six $[Ir(C{\wedge}N)_2(N{\wedge}N)]Cl$ complexes are depicted in Fig. 4, and values of λ_{max} and ε_{max} are given in the experimental section. The intense absorption maxima in the high-energy region arise from spin- and Laporte-allowed C^N and N^N ligand-based $\pi^*{\leftarrow}\pi$ transitions. For each of $[Ir(ppy)_2\{(R)$-**1**$\}]Cl$, $[Ir(ppy)_2\{(S)$-**1**$\}]Cl$, $[Ir(ppy)_2\{(R)$-**3**$\}]Cl$ and $[Ir(ppy)_2\{(S)$-**3**$\}]Cl$, the most intense band appears at λ_{max} = 255 nm. The change in profile of the absorption spectrum and the gain in a maximum at 276 nm on going to $[Ir\{(R)$-**2**$\}_2(bpy)]Cl$ and $[Ir\{(R)$-**4**$\}_2(bpy)]Cl$ corresponds to relocating the ribofuranose-functionality from the bpy to the cyclometallating ligand. The absorption bands in the UV region can be partitioned into those characteristic of C^N ligand-centred (^1LC) transitions (higher energy) and those with larger contributions from N^N ligand-based transitions (~280–330 nm) [24,25]. The weak and broad absorptions in the visible (425 nm for $[Ir(ppy)_2\{(R)$-**1**$\}]Cl$, $[Ir(ppy)_2\{(S)$-**1**$\}]Cl$, $[Ir(ppy)_2\{(R)$-**3**$\}]Cl$ and $[Ir(ppy)_2\{(S)$-**3**$\}]Cl$, and 400 nm for $[Ir\{(R)$-**2**$\}_2(bpy)]Cl$ and

[Ir{(*R*)-**4**}$_2$(bpy)]Cl) arise from charge transfer (^{1}MLCT and ^{1}LLCT) transitions. The shift from 425 nm for the first series to 400 nm for the second pair of compounds is presumably associated with functionalization being on either the C^N (localized on the HOMO) or the N^N ligand (localized on the LUMO) [12].
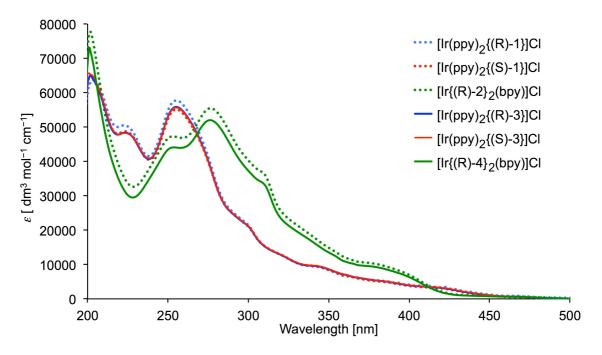

Fig. 4. Solution absorption spectra (in MeOH, 1×10^{-5} mol dm^{-3}) of the [Ir(C^N)$_2$(N^N)]Cl complexes. Dotted curves refer to complexes with acetyl-protected ligands.

Figure 5 shows the emission spectra of MeOH solutions of the six complexes and quantum yields and emission lifetimes for both degassed and non-degassed solutions are given in Table 2. The lowest energy triplet state of an [Ir(C^N)$_2$(N^N)]$^+$ complex is the emitting state, and broad emission bands (Fig. 5) are indicative of dominant charge-transfer (^{3}MLCT and ^{3}LLCT) contributions [12]. For each of [Ir(ppy)$_2${(*R*)-**1**}]Cl, [Ir(ppy)$_2${(*S*)-**1**}]Cl, [Ir(ppy)$_2${(*R*)-**3**}]Cl and [Ir(ppy)$_2${(*S*)-**3**}]Cl, λ_{em}^{max} is in the range 571–576 nm. A shift to lower energy is observed on going to [Ir{(*R*)-**2**}$_2$(bpy)]Cl and [Ir{(*R*)-**4**}$_2$(bpy)]Cl, consistent with the electrochemical band-gap, ΔE (Table 1) which decreases on going from [Ir(ppy)$_2$(N^N)]Cl (N^N = (*R*)-**1**, (*S*)-**1**, (*R*)-**3** and (*S*)-**3**) to

[Ir(C^N)$_2$(bpy)]Cl (C^N = [(R)-**2**]$^-$ and [(R)-**4**]$^-$). Values of λ_{em}^{max} for the latter two complexes (588 and 589 nm) are similar to that of the archetype complex [Ir(ppy)$_2$(bpy)]$^+$ (585 nm) [26].

In degassed solution, the photoluminescence QY values for the series of complexes are similar and are only slightly lower than the 14% reported for [Ir(ppy)$_2$(bpy)][PF$_6$] in deaerated MeCN solution [26]. The introduction of the peripheral ribofuranose groups and the positioning on the bpy or ppy moieties has little effect on the QY. The emission lifetimes of 228–250 ns (Table 2) compare favourably with that of 430 nm for [Ir(ppy)$_2$(bpy)][PF$_6$] (MeCN) [26].

Table 2. Emission maxima (λ_{em}^{max}), quantum yields (QY) and emission lifetimes ($\tau_{1/2}$) of MeOH solutions.

Complex[a]	λ_{em}^{max} / nm	QY / %		$\tau_{1/2}$ / ns	
		Non-degassed	Degassed	Non-degassed	Degassed
[Ir(ppy)$_2$\{(R)-**1**\}]Cl	571	3.0	10.3	71	250
[Ir(ppy)$_2$\{(S)-**1**\}]Cl	576	3.0	9.1	70	228
[Ir\{(R)-**2**\}$_2$(bpy)]Cl	588	2.1	7.4	64	236
[Ir(ppy)$_2$\{(R)-**3**\}]Cl	572	2.9	9.3	68	236
[Ir(ppy)$_2$\{(S)-**3**\}]Cl	572	2.8	9.7	68	241
[Ir\{(R)-**4**\}$_2$(bpy)]Cl	589	2.3	7.7	65	233

[a] λ_{exc} = 280 nm, concentration = 5.0 × 10^{-6} mol dm^{-3}; lifetime detected at 570 nm for [Ir(ppy)$_2$\{(R)-**1**\}]Cl, [Ir(ppy)$_2$\{(S)-**1**\}]Cl, [Ir(ppy)$_2$\{(R)-**3**\}]Cl, [Ir(ppy)$_2$\{(S)-**3**\}]Cl and at 590 nm for [Ir\{(R)-**2**\}$_2$(bpy)]Cl and [Ir\{(R)-**4**\}$_2$(bpy)]Cl.

Fig. 4. Normalized solution emission spectra (in MeOH, 1×10^{-5} mol dm^{-3}) of the [Ir(C^N)$_2$(N^N)]Cl complexes (λ_{exc} = 380 nm, the small band at 760 nm is the first harmonic). Dotted curves refer to complexes with acetyl-protected ligands.

4   Conclusions

In this paper we have described the preparation and characterization of a series of sugar-functionalized luminescent complexes based upon an [Ir(C^N)$_2$(N^N)]$^+$ core. The sugar substituents were introduced on both the C^N (Hppy) and N^N (bpy) ligands. The successful synthesis of these compounds shows that conjugates incorporating the desired functionality can be achieved without developing new strategies. The photophysical and electrochemical properties of the [Ir(C^N)$_2$(N^N)]$^+$ core are unaffected and modulation through substitution of the C^N and N^N ligands conforms with the expected frontier orbital contributions.

Supplementary data online:

Figs. S1–S12 give NMR spectra for the six iridium(III) complexes.

References

[1]   G. Chelucci, Coord. Chem. Rev. 257 (2013) 1887 and references therein.

[2]   K. Ohmatsu, T. Ooi, Tetrahedron Lett. 56 (2015) 2043 and references therein.

[3]   L. Hong, W. Sun, D. Yang, G. Li, R. Wang, Chem. Rev. 116 (2016) 4006 and references therein.

[4]   E.C. Constable, R. Frantz, C.E. Housecroft, J. Lacour, A. Mahmood, Inorg. Chem. 43 (2004) 4817.

[5]   J.-F. Verchère, S. Chapelle, F. Zin and D.C. Crans, Prog. Inorg. Chem. 47 (1998) 837.

[6]   K.K.-W. Lo, Acc. Chem. Res. 48 (2015) 2985.

[7]   W.H.-T. Law, L. C.-C. Lee, M.-W. Louie, H.-W. Liu, T.W.-H. Ang, K.K.-W. Lo, Inorg. Chem. 52 (2013) 13029.

[8]   M.-J. Li, P. Jiao, M. Lin, G.-N. Chen, X. Chen, Analyst 136 (2011) 205.

[9]   A. Maity, J.-S. Choi, T.S. Teets, N. Deligonul, A.J. Berdis, T.G. Gray, Chem. Eur. J. 19 (2013) 15924.

[10] S. Mandal, R. Das, P. Gupta, B. Mukhopadhyay, Tetrahedron Lett. 53 (2012) 3915.

[11] H.-W. Liu, K.Y. Zhang, W.H.-T. Law, K.K.-W. Lo, Organometallics 29 (2010) 3474.

[12] R.D. Costa, E. Ortí, H.J. Bolink, F. Monti, G. Accorsi, N. Armaroli, Angew. Chem. Int. Ed. 51 (2012) 8178.

[13] E.C. Constable, C.E. Housecroft, A. Mahmood, Carbohydrate Res. 343 (2008) 2567.

[14] E.C. Constable, B. Kariuki, A. Mahmood, Polyhedron 22 (2003) 687.

[15] Y.-R. Hong, C. B. Gorman, J. Org. Chem. 68 (2003) 9019.

[16] J. S. Ward, J. M. Lynam, J. W. B. Moir, D. E. Sanin, A. P. Mountford, I. J. S. Fairlamb, Dalton Trans. 41 (2012) 10514.

[17] F. O. Garces, K. A. King, R. J. Watts, Inorg. Chem. 27 (1988) 3464.

[18] S. Sprouse, K. A. King, P. J. Spellane, R. J. Watts, J. Am. Chem. Soc. 106 (1984) 6647.

[19] M. J. Minch Concepts Magn. Reson. 6 (1994) 41.

[20] E.C. Constable, Chem. Soc. Rev. 42 (2013) 1637.

[21] E. Baranoff, B. F. E. Curchod, J. Frey, R. Scopelliti, F. Kessler, I. Tavernelli, U. Rothlisberger, M. Grätzel, M. K. Nazeeruddin, Inorg. Chem. 51 (2012) 215.

[22] C. D. Ertl, J. Cerdá, J. M. Junquera-Hernández, A. Pertegás, H. J. Bolink, E. C. Constable, M. Neuburger, E. Ortí, C. E. Housecroft, RSC Adv. 5 (2015) 42815.

[23] R.D. Costa, E. Ortí, D. Tordera, A. Pertegás, H.J. Bolink, S. Graber, C.E. Housecroft, L. Sachno, M. Neuburger, E.C. Constable, Adv. Energy Mater. 1 (2011) 282.

[24] F. Neve, A. Crispini, S. Campagna, S. Serroni, Inorg. Chem. 38 (1999) 2250.

[25] F. Neve, M. La Deda, F. Puntoriero, S. Campagna, Inorg. Chim. Acta 359 (2006) 1666.

[26] R.D. Costa, E. Ortí, H.J. Bolink, S. Graber, S. Schaffner, M. Neuburger, C.E. Housecroft, E.C. Constable, Adv. Funct. Mater. 19 (2009) 3456.